https://doi.org/10.48048/tis.2024.7702

The Comparison between Energy Density of Blue and Red Light which Activation Silver Nanoparticles to Inhibition *Candida albicans* Biofilms

Pryandi M. Tabaika[1], Sri Dewi Astuty[2,*], Syamsir Dewang[2], Nur Umriani Permatasari[3] and Wahiduddin[4]

1Undergraduate Students of Department of Physics, Faculty of Mathematics and Natural Sciences, Hasanuddin University, South Celebes 90245, Indonesia
[2]Department of Physics, Faculty of Mathematics and Natural Sciences, Hasanuddin University, South Celebes 90245, Indonesia
[3]Department Chemistry, Faculty of Mathematics and Natural Sciences, Hasanuddin University, South Celebes 90245, Indonesia
[4]Faculty of Public Health, Hasanuddin University, South Celebes 90245, Indonesia

([*]Corresponding author's e-mail: dewiastuti@fmipa.unhas.ac.id)

Received: 10 November 2023, Revised: 1 January 2024, Accepted: 8 January 2024, Published: 1 June 2024

Abstract

Photodynamic inactivation (PDI) is a technique to inhibit microbial biofilm growth through the toxicity of Reactive Oxygen Species (ROS) compounds. ROS can be attack membrane, lipids, DNA and nucleic acid then initiate cell necrosis. This study aims to analyze the potential of red and blue LEDs to activating silver nanoparticles (AgNPs) to produce significant amounts of ROS that are believed to be toxic and lethal to *Candida albicans* biofilm cells. The effectiveness of the treatment in this study was evaluated through cell viability represented by Optical Density values and malondialdehyde levels. There were 4 treatment groups used as samples, namely the control group, the photosensitizer group, the light group, and the combination group of light with photosensitizer. The duration of light exposure ranged from 2 to 10 min with a power of 100 MW. The biofilm staining done to detection some indicator as an impact of photodynamic against mortality and survive cell with 2 dyes are XTT assay as cell viability values and the Thiobarbituric Acid Reactive Substances assay for malondialdehyde levels. The results showed that photoinactivation of *Candida albicans* biofilm with the lowest viability occurred in the treatment group of the combination of blue light with AgNPs with an irradiation duration of 10 min, namely 0.076 ± 0.005 and the treatment group of the combination of red light with AgNPs with an irradiation duration of 10 min, namely 0.131 ± 0.021. The data resulted in an inactivation rate of 94.68 ± 0.55 % for blue light and 90.98 ± 0.02 % for red light. The malondialdehyde levels were 1.563 nmol/mL for blue light and 1.514 nmol/mL for red light. The comparison of blue light treatment with red light is based on penetration in the cell, where blue light has low penetration but high energy which gives more opportunities to produce ROS at the triplet level. The combination of blue LED spectrum with AgNPs is highly effective in inactivating the metabolic activity of pathogenic microbial cells.

Keywords: Silver nanoparticles, Red-blue LEDs, Photoinactivation, *Candida albicans* biofilms, XTT assay, Malondialdehyde, Lipid lysis

Introduction

Over the past few decades, *Candida albicans* has become the most common agent causing mucosal and systemic infections, accounting for approximately 70 % of fungal infections worldwide [1,2]. The National Nosocomial Infection Survey (NNIS) revealed that *Candida* spp. ranked as the 4th most common cause of nosocomial bloodstream infections during the 1990 [3,4]. *Candida albicans* is a major contributor to infections in hospitals, especially in the intensive care unit in the incidence of candidemia of 15 % of nosocomial infections, with mortality rates reaching 47 % [5]. One of the important characteristics of *Candida albicans* is its ability to form biofilms as well as pseudo hyphae morphology that can invade deeper tissues on the substrate it occupies, especially in antibiotic-resistant [6].

Biofilms are complex structures consisting of bacterial colonies living in an exopolysaccharide matrix attached to foreign surfaces inside living organisms [7]. Biofilm formation by *Candida albicans* has become a serious concern in the healthcare environment, especially when it comes to the use of medical devices such as catheters, implants, and prostheses. When these surfaces are infected by *Candida albicans* biofilms,

they serve as reservoirs for other pathogenic cells that are difficult to remove. The biofilm matrix becomes a physics and chemical barrier to antibiotic agents resulting in eradication failure. This results in the infection leaving persistent cells in the biofilm and becomes a challenge in clinical management [8,9].

To overcome antibiotic resistance in *Candida albicans*, Photodynamic Inactivation (PDI) has emerged as one of the alternative methods that continues to be developed and modified. PDI involves the use of light that activates photosensitizer compounds to produce oxidative reactions that damage microorganisms [10,11]. The principle of photoinactivation involves the activation of photosensitizer molecules through light absorption and electron transfer to oxygen molecules, resulting in reactive and toxic compounds known as reactive oxygen species (ROS) [12,13].

ROS are chemically active oxygen-containing atoms or groups, including singlet oxygen ($^1O_2$), superoxide anion (O^{2-}), hydroxyl radical (–OH) and hydrogen peroxide (H_2O_2) [14-16]. The toxicity and reactivity of ROS compounds cause damage to microbial cell membranes, inhibit cell division systems, and damage cell DNA chains. Damage to the cell membrane provides an opportunity for photosensitizers to enter the cell, which then damages organelles such as lysosomes, mitochondria, and cell nuclei [13,17]. One indicator of the amount of microbial cell damage due to the influence of ROS is the formation of malondialdehyde (MDA) compounds as a consequence of an inhibited metabolic system. One indicator of the amount of microbial cell damage due to the influence of ROS is the formation of MDA compounds as a consequence of an inhibited metabolic system [18].

The PDI mechanism consists of 3 main components: light, photosensitizer (PS) molecules, and oxygen [19,20]. The choice of light source can determine the success of the PDI mechanism by adjusting the maximum absorption characteristics, of the PS molecule. Maximum absorption at a certain wavelength means that the PS absorbs a significant amount of photon energy and is assumed to provide a higher probability of electron excitation to the triplet state, resulting in singlet oxygen and ROS [13,21].

Before application, the selection of PS requires a number of characterization tests, especially on its physical properties and biological activity. PS is a light-sensitive molecule, which initiates the formation of radical compounds after reacting with oxygen molecules at the triplet level [22]. There are several commonly used organic PS, such as chlorophyll, methylene blue, toluidine blue, malachite green, allyl isothiocyanate and 5-aminolevulinat [23-26]. However, organic PS molecules have a micro-sized structure, making it difficult to penetrate biofilms that are nano-sized or around 50 nm. Therefore, organic PS molecules are less effective for applications in PDI [26,27]. Silver nanoparticle (AgNPs) are one of the interesting nanomaterials in the biomedical world due to their nano size [28]. According to the research of Gibala *et al.* [29], it is proven that nanosilver have antifungal and antibacterial properties, making them potential candidates as photosensitizer agents in PDI mechanisms.

In addition to the PS, the light source is also important to consider to produce optimal photosensitization during PDI. The most commonly used light sources in PDI applications are laser light and LED light. Lasers have the properties of coherent, high-energy and focused or single-point light while LED light has the properties of incoherent, spectrally broad and wide divergence. Therefore, it is less effective in covering the entire surface of the biofilm target simultaneously [30]. LEDs are one of the light sources that are monochromatic and diffuse but have lower energy compared to lasers. LEDs also have the advantage of being an economical light source, easy to assemble and do not produce thermal effects, making them very suitable for use in PDI [31,32].

There have been many publications related to PDI (in other studies use the terms Photodynamic Therapy (PDT) or antimicrobial Photodynamic therapy (aPDT) to describe this mechanism) in recent years. In 2019, Astuty *et al.* [13] used laser diodes and chlorophyll extract from papaya leaves to fight *Candida albicans* fungal infection, resulting in a reduction effect of 32 % (with chlorophyll) and 23 % (without chlorophyll). Furthermore, in the previous year (2018), another study revealed that silver nanoparticle antifungal agents activated by laser diodes can reduce *Candida albicans* biofilms by 64.48 % [26]. In 2020, Mirfasihi *et al.* [33] successfully used chitosan compounds in Photodynamic Therapy (PDT) to treat *Streptococcus mutans* bacteria with a 660 nm laser and 50 MW power. The combination of PDT with chitosan showed the maximum bactericidal effect, followed by PDT for 40 s and the chitosan group ($p < 0.05$). PDT for 30 s showed the minimum bactericidal effect ($p < 0.05$), with a significant comparison ($p < 0.001$).

This study is a development of a previous study, which used AgNPs with a laser light source [26]. This study aims to see the potential of AgNPs to produce a number of radical compounds after being activated with red and blue LED light in the inhibition of *Candida albicans* biofilm growth. The advantage of this study is to increase the oxygen concentration on the biofilm surface before irradiation, with the intention that the production of singlet oxygen is more dominant than other radical compounds.

Materials and methods

Synthesis and characterization of silver nanoparticles

Synthesis of silver nanoparticles done with methods referred to (**Figure 1(a)**). It requires 150 mL of 1 mM silver nitrate ($AgNO_3$) solution, which is heated to boiling using a hotplate. Then, 5 mL of 1 % trisodium citrate is added drop by drop to the solution while stirring using a magnetic stirrer until the color of the solution changes from yellow to brown [26]. Afterward, the solution is left to cool down to room temperature. Next, the synthesized AgNPs solution is characterized to determine its optical properties using UV-VIS spectroscopy (Shimadzu-03972) with a wavelength range of 300 - 700 nm.

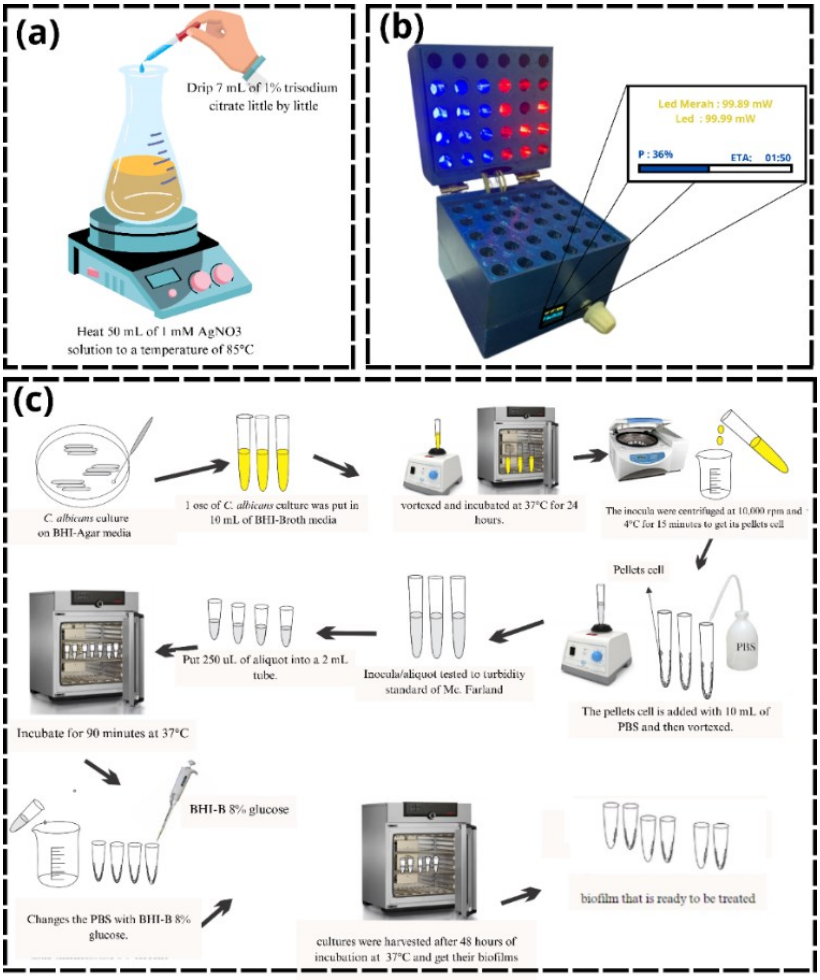

Figure 1 Material and methods (a) Silver nanoparticle synthesis method, (b) Illumination instrument, and (c) Method for creating *Candida albicans* biofilm from within a 2 mL tube.

Light source

The light sources used in this study are red and blue LEDs controlled by a microcontroller system with 5 types of energy associated with irradiation time with an interval of 2 min. The power regulated in this study used a power of 100 MW. $I_{absorbed}$ (MW/cm^2) is the intensity of light absorbed by AgNPs which represents the characteristics of the absorption rate of AgNPs at the wavelength corresponding to the light source used. Furthermore, this parameter is used to determine the E_n (mJ/cm^2) which is the light energy density of red and blue LEDs based on changes in irradiation time (s) varied in the study. The equation to calculate the LED energy density based on the irradiation time and intensity absorbed by both LEDs towards AgNPs is [34]:

$$E_n = I_{absorbed} \times t \quad (1)$$

The intensity and energy density used in this study are shown in the following table.

Table 1 Data of light parameters this research.

Treatment group	LEDs Intensity (MW/cm^2)		LEDs Intensity absorbed by AgNPs (MW/cm^2)		Time irradiation (s)	Energy density LEDs (mJ/cm^2)	
	Red LED	Blue LED	Red LED	Blue LED		Red LED	Blue LED
L1					120	4.92	16.56
L2					240	9.84	33.12
L3	0.179	0.141	0.041	0.138	360	14.76	49.68
L4					480	19.68	66.24
L5					600	24.60	82.80

Growth biofilm in an Eppendorf tube

Samples of *Candida albicans* were obtained from the microbiology laboratory collection at the Faculty of Medical, Universitas Muslim Indonesia (UMI) Makassar, Indonesia. Sample collection was conducted using standard methods in the field of microbiology for fungal organisms. Subsequently, the samples were cultured on Brain Heart Infusion Agar/BHI-A (Oxoid, England, UK) and inoculated in Brain Heart Infusion Broth/BHI-B (Oxoid, England, UK) for 24 h. To induce biofilm formation, the inoculum was diluted with sterile Phosphate Buffered Saline (PBS) until it reached an optical density of OD_{600nm} = 0.570 (approximately 3×10^8 CFU/mL). The treatments were divided into 4 main groups, as shown in **Figure 2**. Biofilm growth was induced using Brain Heart Infusion Broth supplemented with 8 % glucose (BHI-B 8 % glucose) and incubated for 48 h.

Experimental design

Before incubation AgNPs in biofilm are flowed with oxygen gas for 30 s with a discharge of 1 L/min. The distance between the LED light and the sample surface was set at 3 cm. The treatments were divided into 4 main groups, as shown in **Figure 2**.

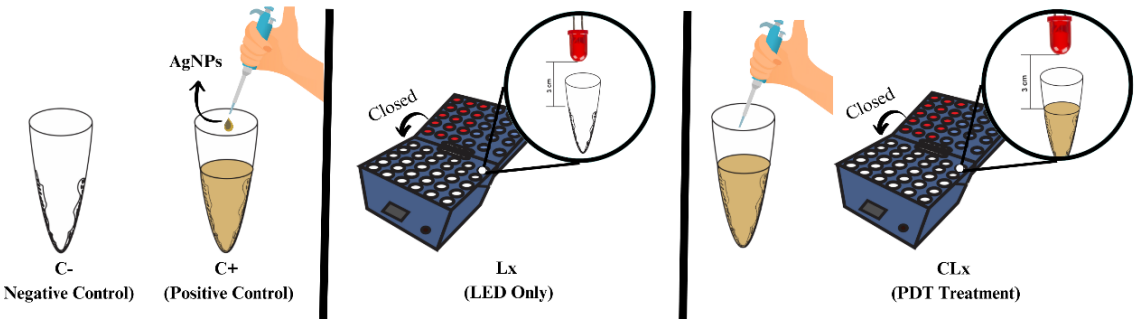

Figure 2 The experimental treatment groups design base on sample groups codes.

All treatment groups were made with 3 replicates and the samples for each treatment included 2 types of red and blue LEDs. Treatment codes were made in 4 groups, namely C– (Biofilm oxygenated), C+ (biofilm oxygenated treated with AgNPs), Lx (biofilm oxygenated irradiated with LEDs only), and CLx (Biofilm treated with PDI or a combination of LEDs and AgNPs). So, for Lx and CLx (x is 1, 2, 3, 4 and 5 which indicates the irradiation time of 2, 4, 6, 8 and 10 min, respectively). Testing the effect of PDI was carried out in 2 stages, namely the namely the tetrazolium dye, 2,3-bis- (2-methoxy-4-nitro-5-sulphenyl)-(2H)-tetrazolium-5-carboxanilide (XTT) test and the MDA level test. The XTT test aims to detect cells that are still alive or that are still actively metabolizing, while the MDA test aims to detect the number of cells that have died due to ROS attack on bacterial cells. The MDA assay is also used as an approach to estimate the amount of ROS formed during the duration of irradiation.

Detection cell by XTT assay and TBARS methods

The cell viability of the samples after photoinactivation treatment was assessed using the XTT staining method [13,35,36]. For the XTT staining assay, the photoinactivated biofilm was stained with 80 µL of 1 mg/mL XTT, 4 µL of 20 mg/mL menadione and 316 µL of sterile PBS. After staining, the biofilm was incubated in the dark for 90 min at 37 °C. A total of 100 µL of XTT staining aliquot was transferred to a new microplate and analyzed using an ELISA reader at a 490 nm wavelength. The ratio between the viability value of the control group ($OD_{control}$) to the viability of the treatment group ($OD_{treatment}$) is expressed as the photoinactivation effect or percentage inhibition (% Inhibition). Subsequently, the obtained data were used to calculate the percentage of cell death using the following equation [37].

$$\%\ inhibition = \left|\frac{OD_{control} - OD_{treatment}}{OD_{control}}\right| \times 100 \quad (2)$$

The levels of malondialdehyde (MDA) produced after treatment in **Figure 2** were assayed using the Thiobarbituric Acid Reactive Substances (TBARS) method [13,36]. Diluted 0.5 mL filtrate of the photoinactivated biofilm (mixed with distilled water) was then centrifuged at 4 °C for 10 min, then mixed with 0.5 mL sterile PBS, 1 mL 20 % trichloroacetic acid and 1 mL 0.67 % Thiobarbituric acid, followed by homogenization. Next, the homogenate was heated in a water bath at 80 °C for 15 min and cooled at room temperature for 60 min. The absorbance of the filtrate was read at a wavelength of 532 nm, and the MDA content was determined after making a standard curve using the standard MDA compound, TEP (1,1,3,3-tetraethoxypropane). The linearity equation of the TEP standard curve used: 0.6373x - 0.7972 (data not shown). The equation can then be calculated MDA levels using the following equation [13]:

$$MDA\ level\left(\frac{\text{nmol}}{\text{mL}}\right) = \frac{y-b}{a} \quad (3)$$

Notes*: a = 0.6373; b = 0.7972; y = absorbance of the sample after staining with TBARS method**.**

Statistical analysis

All data were statistically analyzed using SPSS 26.0 through One-way Analysis of Variance (ANOVA) and Tukey's analysis at a confidence level of 0.05.

Results and discussion

Characteristics of silver nanoparticle photosensitizer

AgNPs photosensitizer was synthesized by reducing $AgNO_3$ using the reductant trisodium citrate ($Na_3C_6H_5O_7$). The absorption spectrum of AgNPs was measured using a UV-VIS spectrophotometer with a wavelength range of 300 - 700 nm. The full width at half maximum (FWHM) of AgNPs is so wide it indicates that the solution has many absorption spectra (not specific). The maximum absorption peak of the solution at a wavelength of 433 nm is shown in **Figure 3**.

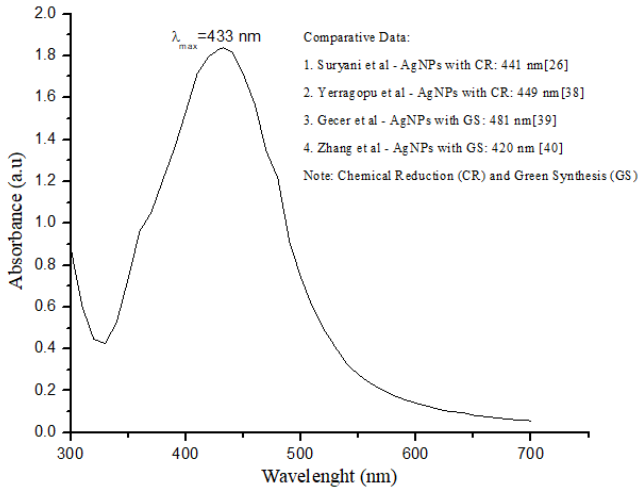

Figure 3 The absorption spectrum of silver nanoparticles (AgNPs).

Figure 3 displays the absorbance spectrum of the AgNPs solution in the wavelength range of 300 - 700 nm. The maximum absorption wavelength is lower than the value obtained by Astuti *et al*. [26] at 441 nm, Yerragopu *et al.* [38] at 449 nm, Gecer *et al.* [39] at 481 nm, but higher than the reference produced by Zhang which is at λmax at 420 nm [40]. The references compared above are spectra of AgNPs prepared using chemical reduction and green synthesis methods that produce differences in maximum absorption wavelengths. The differences obtained are thought to be influenced by preparation and synthesis process factors, namely unstable heating temperature, type of chemical reductant, duration of color change during AgNPs synthesis.

The irradiation sources used in this study are red and blue LEDs which are at wavelengths of 450 nm and 620 nm, respectively. Based on the profile in **Figure 3** AgNPs when absorbing red LED light has an absorption of 0.112 and if activated with blue LED then the absorption value is 1.711. This data is used to obtain an estimate of the % absorption of AgNPs to both light sources, namely red and blue LEDs (as calculated in the appendix) with values of 22.37 and 98.05 %, respectively.

The development of generation III photosensitizers shows a significant shift in focus towards enhancing light absorption to improve PDI efficiency [41] This generation of photosensitizers is designed with optical and photophysical properties in mind that can be optimised, particularly in the context of enhancing the desired photochemical response. One of the unique characteristics of silver nanoparticles (AgNPs) is that they have only one wavelength maximum in the absorption spectrum. This means that the optical properties of AgNPs can be directed to absorb light at specific wavelengths, which can be optimised to achieve maximum therapeutic response in photodynamic therapy. AgNPs also show great potential as nanomolecules that can be effectively applied to microorganisms, especially to candida albicans which has nano-sized pores [26].

Efficacy of PDI to *Candida albicans* biofilms

Figures 4(a) - 4(b) display the decrease in cell viability after photoinactivation treatment with blue LED (**Figure 4**) and red LED (**Figure 5**) compared to the control group. The gray line curve is the optical turbidity value of the nanoparticles (AgNps)-treated group; the red line curve represents the optical turbidity value of the LED-only treated group, and the red and blue dashed curves show the turbidity value of the LED-treated group with AgNPs.

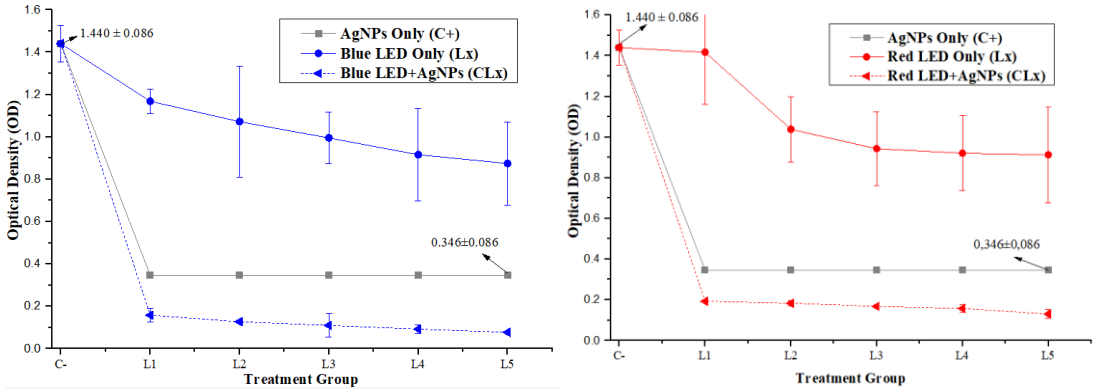

Figure 4 The Viability of *Candida albicans* biofilms (a) with blue LED; (b) with Red LED.

The AgNPs treatment group is used as an antifungal control treatment group which can be seen that AgNPs do have quite high antifungal properties as evidenced by the low optical density value. This indicates that quite a lot of microorganism cells (*Candida albicans*) died due to the antifungal properties of AgNPs. The turbidity value for the AgNPs treatment group was 0.346 ± 0.086 with an inactivation effect of about 75 %.

The photoinactivation effect of the 2 different light treatments with AgNPs or without AgNPs showed a decrease in cell viability along with the length of exposure time given. The optical density value showed that the irradiation group using blue LED was lower than the red LED treatment group. Based on **Figure 4(a)**, it can be seen that the decrease in cell viability value from the negative control group which is 1.440 ± 0.086 to the blue LED only treatment group decreased the average OD value from (1.168 ± 0.058) to (0.874 ± 0.122) and for the combination of blue LED with AgNPs photosensitizer decreased the average OD value to (0.158 ± 0.033) to (0.077 ± 0.005). Similarly, **Figure 4(b)**. the red LED only treatment group

decreased the average OD value from (1.417 ± 0.257) to (0.913 ± 0.236) and for the combination of red LED with AgNPs photosensitizer decreased the average OD value from (0.193 ± 0.008) to (0.131 ± 0.021). This is because the longer the exposure time given, the greater the radiation energy from the LED so that it can be assumed that there are more radical compounds or ROS.

The optical turbidity value shows that the red LED treatment group is lower than the blue LED treatment group. From the 2 curves above, it can also be seen that the longer the exposure time given, the lower the optical turbidity value. This is because there are fewer live *Candida albicans* cells. Based on the optical turbidity values of both treatment groups using red and blue LEDs (**Figures 4(a) - 4(b)**), the inhibition effectiveness can be calculated using Eq. (1) (Formulated in the method).

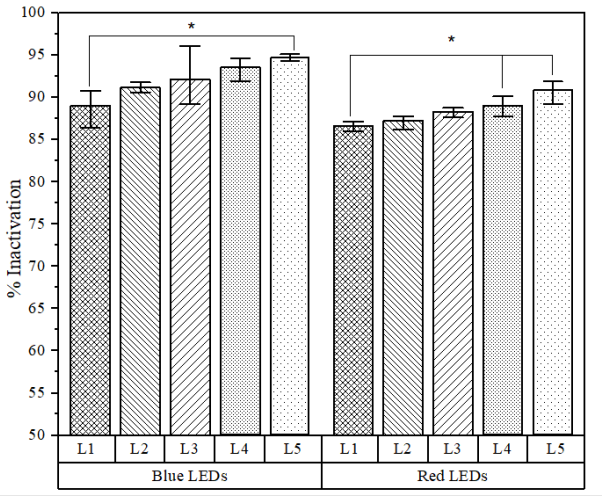

Figure 5 The Inhibition Effect for Groups of the LED with AgNPs Treatment.
Note: * Shows significant level in ANOVA one way test of $p < 0.05$.

Figure 5 displays the comparison data between the treatment groups using LED and the addition of AgNPs from the treatment groups using 2 light treatments (red and blue LEDs). The histogram curve using red LED represents the red histogram, and blue LED treatment represents the blue histogram. The data in **Figure 5**. also displays the comparison of irradiation energy to the % inhibition of *Candida albicans* biofilm. The results of the inhibition calculation show that the minimum inactivation percentage is at an energy density of 11.92 J/cm^2, which is 86.60 and 89.03 % for LEDs at red and blue wavelengths, respectively. An energy density of 59.54 J/cm^2 is the maximum percentage of 5 energy density variations, with inactivation percentages for red and blue wavelength LEDs at 90.90 and 94.65 %, respectively. The results of statistical analysis showed that photoinactivation treatment using a blue LED with AgNPs from L1 was only significant ($p < 0.05$) to L5, while irradiation using a red LED with AgNPs increased significantly from L1 to L4 and L5.

The results obtained from this study are not different from those reported by Maytin *et al.* [42] comparing blue and red light ($p = 100$ MW) with the addition of 5-aminolevulinate for basal cell carcinoma, the data shown shows that the maximum effectiveness is obtained using blue light by 98 %. This data also correlates with the data reported by Jamali *et al.* [43] using 5-aminolevulinic, explaining that the use of blue LEDs is more effective than conventional red LEDs on human glioma cell lines. However, this is inversely proportional to the data reported by Astuty *et al.* [13] obtained the maximum value using a red luminous laser of 32 % and a blue laser of 25 %, this is because the irradiation time used for the red laser is longer than the blue laser.

Photoinactivation of *C. albicans* biofilm has previously been investigated by Leonel *et al.* [44] Investigating the effect of Methylene Blue (MB) concentration and fluence on the percentage of biofilm inhibition, data obtained that the percent inhibition of *Candida albicans* biofilm for MB 0.02 mg/mL, observed inhibition in biofilm formation of 58, 70 and 74 %, using fluence of (10, 20 and 30) J/cm^2, respectively. Also, biofilm inhibition for MB concentrations of (0.01, 0.02 and 0.05) mg/mL of 54, 66 and 55 % was observed. Photoinactivation data was also investigated by Astuti *et al.* [26] to see the effect of laser with AgNPs to reduce *Candida albicans* biofilms and obtained a % reduction of 64.48 ± 0.07 % with an energy of 6.13 ± 0.002 J/cm^2. This study obtained higher success reaching 94.65 % which was thought

to be due to the higher concentration of AgNPs. This is in accordance with research data reported by Ahamad *et al*. [45] Reporting that the concentration of AgNPs will affect the number of dead biofilm cells.

Malondialdehyde content analysis

In photoinactivation, radical compounds are derived from the chemical reaction between the sensitizer and oxygen molecules present around the cell during the photoinactivation process. This has the potential to cause necrosis in microbes due to cell lipid peroxidation. Radical compounds that accumulate in *Candida albicans* cells can result in increased levels of MDA. To measure MDA levels, Trichloroacetic Acid (Merck) and Thiobarbituric Acid (Merck) reagents are used. Previously, it was necessary to find the standard concentration of MDA as a reference to calculate the MDA content of the tested sample.

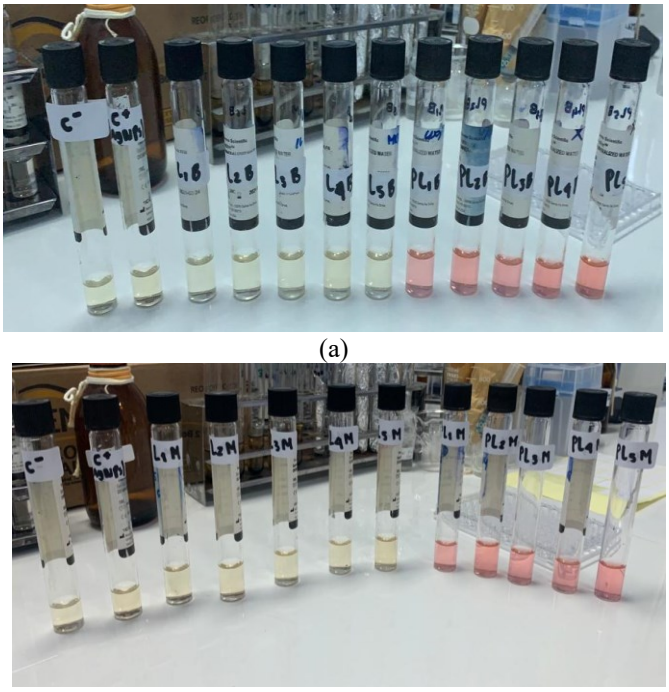

(a)

(b)

Figure 6 Visualization colour to identify MDA level in the samples after TBARS staining from both treatments irradiation with (a) Blue LEDs; (b) Red LEDs.

Measurement of MDA levels in *Candida albicans* biofilm after photoinactivation is used as an indicator of the amount of ROS compounds accumulated in the biofilm tissue. The more pinkish red color means the more MDA levels. Samples for each treatment group for testing MDA levels can be seen in **Figure 6**.

Figure 6 shows the gradation of solution color in each treatment with the highest degree indicated by pink color. Some solutions showed a clear cloudy to pink color, but some solutions did not show a real color but the absorbance measurement results increased indicating the turbidity that occurred compared to the negative control. The figure shows that the treatment groups using PS (AgNPs) with LED irradiation all produce a pink color which is assumed to contain many radical compounds.

Malondialdehyde compounds are produced from the mechanism of lipid peroxidation of *Candida albicans* cell membranes caused by radical compounds or ROS. The accumulation of MDA levels in biofilms is extracted by adding trichloroacetic acid and thiobarbituric acid reagents. MDA compounds in biofilms are an indicator of the number of cells that experience lysis and it is assumed that one ROS attack causes one cell to die. The accumulation of MDA levels was done by measuring the absorbance of the sample using a UV-VIS spectrophotometer. Absorbance or intensity measurements for each treatment group were read at a filter of wavelength of 532 nm. After that, MDA levels were calculated using the TEP calibration curve to obtain the data shown in **Table 2** below.

Table 2 Intensity of TBARS staining degree of all the samples to determine MDA value concentration.

Treatment Groups	Intensity		MDA (nmol/mL)	
	Red LEDs	**Blue LEDs**	**Red LEDs**	**Blue LEDs**
C–	0.0440 ± 0.0010	0.0440 ± 0.0010	1.3199 ± 0.0016	1.3199 ± 0.0016
C+	0.0477 ± 0.0012	0.0477 ± 0.0012	1.3257 ± 0.0024$^{(a)}$	1.3257 ± 0.0024$^{(a)}$
L_1	0.0550 ± 0.0010	0.0613 ± 0.0005	1.3372 ± 0.0016$^{(b)}$	1.3471 ± 0.0009$^{(b)}$
L_2	0.0573 ± 0.0006	0.0630 ± 0.0014	1.3409 ± 0.0009$^{(b)}$	1.3498 ± 0.0027$^{(b)}$
L_3	0.0597 ± 0.0006	0.0637 ± 0.0005	1.3445 ± 0.0009$^{(b)}$	1.3508 ± 0.0009$^{(b)}$
L_4	0.0627 ± 0.0015	0.0663 ± 0.0025	1.3492 ± 0.0024$^{(b)}$	1.3550 ± 0.0048$^{(b)}$
L_5	0.0637 ± 0.0006	0.0690 ± 0.0008	1.3508 ± 0.0009$^{(b)}$	1.3592 ± 0.0016$^{(b)}$
PL_1	0.2030 ± 0.0026	0.2813 ± 0.0021	1.5694 ± 0.0042$^{(b)}$	1.6923 ± 0.0039$^{(b)}$
PL_2	0.2317 ± 0.0029	0.3330 ± 0.0008	1.6144 ± 0.0045$^{(b)}$	1.7734 ± 0.0016$^{(b)}$
PL_3	0.2783 ± 0.0006	0.3650 ± 0.0008	1.6876 ± 0.0009$^{(b)}$	1.8236 ± 0.0016$^{(b)}$
PL_4	0.3087 ± 0.0012	0.3773 ± 0.0012	1.7352 ± 0.0018$^{(b)}$	1.8430 ± 0.0024$^{(b)}$
PL_5	0.3533 ± 0.0015	0.3803 ± 0.0078	1.8053 ± 0.0024$^{(b)}$	1.8477 ± 0.0149$^{(b)}$

Note: Index after SD on the data represented by "(a)" was no difference significant compared control (C–) with ($p > 0.05$) and "(b) was other with ($p < 0.05$).

Table 2 Shows the value of MDA levels from photoinactivation treatment using red LED and blue LED. The value of MDA levels using blue LED for irradiation without PS (AgNPs) has MDA levels between 1.3472 ± 0.0009 to 1.3592 ± 0.0016 nmol/mL and for irradiation with PS (AgNPs) has MDA levels between 1.6923 ± 0.0039 to 1.8477 ± 0.0149 nmol/mL. While the value of MDA levels using red LED for irradiation without PS (AgNPs) has MDA levels between 1.3372 ± 0.0016 to 1.3508 ± 0.0009 nmol/mL and for irradiation with PS (AgNPs) has MDA levels between 1.5694 ± 0.0042 to 1.8053 ± 0.0024 nmol/mL.

The measurement of malondialdehyde levels showed that the LED group without AgNPs was lower than the combination group of light and AgNPs. The negative control treatment group also contained MDA levels which were thought to be due to the biofilm lipid peroxidation process caused by the presence of toxic compounds produced by *Candida albicans* cells or derived from the reaction between Thiobarbituric acid reagent and *Candida albicans* cell survival. The AgNPs treatment group also increased MDA levels compared to the negative control. The increase in MDA levels for the AgNPs group was due to the antifungal properties of AgNPs. MDA levels continued to increase for treatment groups that were irradiated using light. When compared to the treatment of red and blue LED light, the MDA value was so high for the irradiation group using blue LED, which is in accordance with the decreasing optical density data.

Cell viability tests and malondialdehyde levels in biofilms for treatments with AgNPs or C+ treatment showed that AgNPs were able to reduce the OD value significantly ($p < 0.05$). OD data for the C+ treatment is in line with research reported by Jalal *et al.* [46], which concluded that AgNPs can be used as a promising antifungal drug to prevent the development of pathogenesis in *Candida* spp. This is reinforced by the data reported by Arsène *et al.* [47] which also concluded that the synthesized AgNPs showed excellent antifungal activity against *Candida albicans* tested. This discovery explains that AgNPs have antifungal properties because AgNPs are able to penetrate the outer membrane, accumulate in the inner membrane where adhesion of nanoparticles to cells results in destabilization and damage, increasing membrane permeability and inducing leakage of cellular content [48]. More *et al.* [49] also explained that AgNPs cause oxidative stress, protein dysfunction, membrane disruption and DNA damage in bacteria, which ultimately leads to the death of microorganisms. From all the studies above, they only used AgNPs to treat microorganism cells.

One of the advantages of this finding is that it combines with low-energy light, namely LED. It is hoped that in addition to the toxic effects of the natural properties of AgNPs, the combination with the light will produce even more toxic effects. Both of the tests above show that their inhibition reached 94 %. When AgNPs particles that are already toxic interact with photons, they will produce singlet oxygen radical compounds and ROS. So, the microorganism cells not only die because of the toxicity of the AgNPs but

also because of the attack of ROS. The formation of ROS from photoinactivation treatment is effective if adjusted to the maximum absorbance of the photosensitizer molecule. when many photons are absorbed by the PS molecule, it will cause the electrons of the PS molecule to be excited to the singlet state level and internal converter and intersystem crossing to the triplet state occurs. in this triplet state, oxygen will get electron transfer and energy transfer. If oxygen in the triplet state gets energy transfer, it will form a singlet state ($^1O_2$) and if the electron transfer will form ROS such as hydroxyl radical (–OH) and hydrogen peroxide (H_2O_2) and others. The treatment done with red and blue LEDs shows that the blue treatment group has the most effective tendency. The data also showed that the longer the irradiation time, the higher the MDA levels. The report of our study, in line with research reported by Rahmadan *et al.* [35] and Zain *et al.* [36].

Conclusions

The synthesis of AgNPs was developed for the application of photosensitizing agents in photodynamic inactivation. This potential was illustrated through indicators of the number of surviving cells and the amount of cell MDA compounds due to cell lysis. The characteristics of AgNPs and MDA content were investigated through spectrum analysis while OD values were measured with an ELISA reader. Combination with a low-energy light source such as LED resulted in a potential inhibition of up to 94.64 % of biofilm microbial cell death. The test results, which were statistically processed, showed that the decrease in cell viability and MDA levels were significantly different ($p < 0.05$) from the combination treatment of AgNPs and LEDs against the negative control. The maximum absorption of AgNPs which absorbs photons in the 433 nm region (blue spectrum) was found to be in accordance with photoinactivation optimization using blue LEDs. This suggests that AgNPs as a photosensitizing agent in PDI has the potential to be activated with blue light in the future.

Acknowledgements

The author thanks LP2M Hasanuddin University, Indonesia for funding this research as a part of Grant Penelitian Fundamental Kolaborasi (PFK) 2023 with contract No. 000323/UN4.22/PT.01.03/2023, also to Mr. Heryanto as for his coaching publication.

References

[1] J Talapko, M Juzbašić, T Matijević, E Pustijanac, S Bekić, I Kotris and I Škrlec. *Candida albicans*-the virulence factors and clinical manifestations of infection. *J. Fungi* 2021; **7**, 79.
[2] HOJ Morad, AM Wild, S Wiehr, G Davies, A Maurer, BJ Pichler and CR Thornton. Pre-clinical imaging of invasive candidiasis using ImmunoPET/MR. *Front. Microbiol.* 2018; **9**, 1996.
[3] T Atriwal, K Azeem, FM Husain, A Hussain, MN Khan, MF Alajmi and M Abid. Mechanistic understanding of candida albicans biofilm formation and approaches for its inhibition. *Front. Microbiol.* 2021; **12**, 638609.
[4] MB Lohse, M Gulati, AD Johnson and CJ Nobile. Development and regulation of single- and multi-species *Candida albicans* biofilms. *Nat. Rev. Microbiol.* 2018; **16**, 19-31.
[5] EWL Chow, LM Pang and Y Wang. From Jekyll to Hyde: The yeast-hyphal transition of *Candida albican*. *Pathogens* 2021; **10**, 859.
[6] PPD Barros, RD Rossoni, CMD Souza, L Scorzoni, JDC Fenley and JC Junqueira. Candida biofilms: An update on developmental mechanisms and therapeutic challenges. *Mycopathologia* 2020; **185**, 415-24.
[7] S Sharma, J Mohler, SD Mahajan, SA Schwartz, L Bruggemann and R Aalinkeel. Microbial biofilm: A review on formation, infection, antibiotic resistance, control measures, and innovative treatment. *Microorganisms* 2023; **11**, 1614.
[8] M Gulati and CJ Nobile. Candida albicans biofilms: Development, regulation, and molecular mechanisms. *Microb. Infect.* 2016; **18**, 310-21.
[9] R Pereira, RODS Fontenelle, EHSD Brito and SMD Morais. Biofilm of *Candida albicans*: Formation, regulation and resistance. *J. Appl. Microbiol.* 2021; **131**, 11-22.
[10] T Maisch. Resistance in antimicrobial photodynamic inactivation of bacteria. *Photochemical Photobiological Sci.* 2015; **14**, 1518-26.
[11] B Pucelik and JM Dąbrowski. Photodynamic inactivation (PDI) as a promising alternative to current pharmaceuticals for the treatment of resistant microorganisms. *Adv. Inorg. Chem.* 2022; **79**, 65-103.
[12] JM Dąbrowski. Reactive oxygen species in photodynamic therapy: Mechanisms of their generation and potentiation. *Adv. Inorg. Chem.* 2017; **70**, 343-94.

[13] SD Astuty, Suhariningsih, A Baktir and SD Astuti. The efficacy of photodynamic inactivation of the diode laser in inactivation of the *Candida albicans* biofilms with exogenous photosensitizer of papaya leaf chlorophyll. *J. Lasers Med. Sci.* 2019; **10**, 215-24.
[14] PL Lam, RSM Wong, KH Lam, LK Hung, MM Wong, LH Yung, YW Ho, WY Wong, DKP Hau, R Gambari and CH Chui. The role of reactive oxygen species in the biological activity of antimicrobial agents: An updated mini review. *Chem. Biol. Interact.* 2020; **320**, 109023.
[15] A Xie, H Li, Y Hao and Y Zhang. Tuning the toxicity of reactive oxygen species into advanced tumor therapy. *Nanoscale Res. Lett.* 2021; **16**, 142.
[16] F Collin. Chemical basis of reactive oxygen species reactivity and involvement in neurodegenerative diseases. *Int. J. Mol. Sci.* 2019; **20**, 2407.
[17] CA Juan, JMPDL Lastra, FJ Plou and E Pérez-Lebeña. The chemistry of reactive oxygen species (ROS) revisited: Outlining their role in biological macromolecules (DNA, lipids and proteins) and induced pathologies. *Int. J. Mol. Sci.* 2021; **22**, 4642.
[18] M Morales and S Munné-Bosch. Malondialdehyde: Facts and artifacts. *Plant Physiol.* 2019; **180**, 1246-50.
[19] L Sheng, X Li and L Wang. Photodynamic inactivation in food systems: A review of its application, mechanisms, and future perspective. *Trends Food Sci. Tech.* 2022; **124**, 167-81.
[20] M Gallardo-Villagrán, DY Leger, B Liagre and B Therrien. Photosensitizers used in the photodynamic therapy of rheumatoid arthritis. *Int. J. Mol. Sci.* 2019; **20**, 3339.
[21] Y Li, X Zhang and D Liu. Recent developments of perylene diimide (PDI) supramolecular photocatalysts: A review. *J. Photochem. Photobiol. C Photochem. Rev.* 2021; **48**, 100436.
[22] MCS Vallejo, NMM Moura, MAF Faustino, A Almeida, I Gonçalves, VV Serra and MGPMS Neves. An insight into the role of non-porphyrinoid photosensitizers for skin wound healing. *Int. J. Mol. Sci.* 2021; **22**, 234.
[23] J Shen, Q Liang, G Su, Y Zhang, Z Wang, C Baudouin and A Labbé. *In vitro* effect of toluidine blue antimicrobial photodynamic chemotherapy on *Staphylococcus epidermidis* and *Staphylococcus aureus* isolated from ocular surface infection. *Translational Vis. Sci. Tech.* 2019; **8**, 45.
[24] E Polat and K Kang. Natural photosensitizers in antimicrobial photodynamic therapy. *Biomedicines* 2021; **9**, 584.
[25] HA Choi, DE Cheong, HD Lim, WH Kim, MH Ham, MH Oh, Y Wu, HJ Shin and GJ Kim. Antimicrobial and anti-biofilm activities of the methanol extracts of medicinal plants against dental pathogens streptococcus mutans and *Candida albicans*. *J. Microbiol. Biotechnol.* 2017; **27**, 1242-8
[26] SD Astuti, PS Puspita, AP Putra, AH Zaidan, MZ Fahmi, A Syahrom and Suhariningsih. The antifungal agent of silver nanoparticles activated by diode laser as light source to reduce C. albicans biofilms: An *in vitro* study. *Lasers Med. Sci.* 2019; **34**, 929-37.
[27] TO Peulen and KJ Wilkinson. Diffusion of nanoparticles in a biofilm. *Environ. Sci. Tech.* 2011; **45**, 3367-73.
[28] L Xu, YY Wang, J Huang, CY Chen, ZX Wang and H Xie. Silver nanoparticles: Synthesis, medical applications and biosafety. *Theranostics* 2020; **10**, 8996-9031.
[29] A Gibała, P Żeliszewska, T Gosiewski, A Krawczyk, D Duraczyńska, J Szaleniec, M Szaleniec and M Oćwieja. Antibacterial and antifungal properties of silver nanoparticles-effect of a surface-stabilizing agent. *Biomolecules* 2021; **11**, 1481.
[30] M Piksa, C Lian, IC Samuel, KJ Pawlik, IDW Samuel and K Matczyszyn. The role of the light source in antimicrobial photodynamic therapy. *Chem. Soc. Rev.* 2023; **52**, 1697-722.
[31] N Rasiukevičiūtė, A Brazaitytė, V Vaštakaitė-Kairienė, A Kupčinskienė, P Duchovskis, G Samuolienė and A Valiuškaitė. The effect of monochromatic LED light wavelengths and photoperiods on botrytis cinerea. *J. Fungi* 2021; **7**, 970.
[32] MM Kim and A Darafsheh. Light sources and dosimetry techniques for photodynamic therapy. *Photochem. Photobiol.* 2020; **96**, 280-94.
[33] A Mirfasihi, BM Afzali, HE Zadeh, K Sanjari and M Mir. Effect of a combination of photodynamic therapy and chitosan on *Streptococcus mutans* (an *in vitro* study). *J. Lasers Med. Sci.* 2020; **11**, 405-10.
[34] SD Astuti, IB Utomo, EM Setiawatie, M Khasanah, H Purnobasuki, D Arifianto and KA Alamsyah. Combination effect of laser diode for photodynamic therapy with doxycycline on a wistar rat model of periodontitis. *BMC Oral Health* 2021; **21**, 80.
[35] S Ramadhana, SD Astuty, B Bannu, E Enggrianti and RR Wahyudi. Physicochemical study of castor leaf (*Jatropha curcas* L.) and lapaya leaf (*Carica papaya* L.) extract and their application as

photosensitizer agents in antimicrobial photodynamic therapy system to *Staphylococcus epidermidis* biofilm. *AIP Conf. Proc.* 2023; **2719**, 020018.

[36] M Zain, SD Astuty, S Dewang, B Armynah, RR Wahyudi and S Ramadhana. Analysis of the changes power output and energy dose to green laser against OD and MDA values after photoinactivation at *Candida albicans* and *Staphyloccocus epidermidis* associate biofilms. *AIP Conf. Proc.* 2023; **2719**, 020006.

[37] SD Astuty, S Dewang, FA Tasmara and RR Wahyudi. Activity detection of noni leaf (*Morinda citrifolia* L.) chlorophyll extract through the photoinactivation to reducing Streptococcus mutans cells using XTT assay method. *AIP Conf. Proc.* 2022; **2663**, 6.

[38] PS Yerragopu, S Hiregoudar, U Nidoni, KT Ramappa, AG Sreenivas and SR Doddagoudar. Chemical synthesis of silver nanoparticles using tri-sodium citrate, stability study and their characterization. *Int. Res. J. Pure Appl. Chem.* 2020; **21**, 37-50.

[39] EN Gecer, R Erenler, C Temiz, N Genc and I Yildiz. Green synthesis of silver nanoparticles from *Echinacea purpurea* (L.) Moench with antioxidant profile. *Particulate Sci. Tech.* 2022; **40**, 50-7.

[40] H Zhang, M Peng, T Cheng, P Zhao, L Qiu, J Zhou, G Lu and J Chen. Silver nanoparticles-doped collagen-alginate antimicrobial biocomposite as potential wound dressing. *J. Mater. Sci.* 2018; **53**, 14944-52.

[41] IS Mfouo-Tynga, LD Dias, NM Inada and C Kurachi. Features of third generation photosensitizers used in anticancer photodynamic therapy: Review. *Photodiagnosis Photodynamic Ther.* 2021; **34**, 102091.

[42] EV Maytin, U Kaw, M Ilyas, JA Mack and B Hu. Blue light versus red light for photodynamic therapy of basal cell carcinoma in patients with Gorlin syndrome: A bilaterally controlled comparison study. *Photodiagnosis Photodynamic Ther.* 2018; **22**, 7-13.

[43] Z Jamali, SM Hejazi, SM Ebrahimi, H Moradi-Sardareh and M Paknejad. Effects of LED-based photodynamic therapy using red and blue lights, with natural hydrophobic photosensitizers on human glioma cell line. *Photodiagnosis Photodynamic Ther.* 2018; **21**, 50-4.

[44] LDC Leonel, ML Carvalho, BMD Silva, S Zamuner, C Alberto-Silva and MS Costa. Photodynamic antimicrobial chemotherapy (PACT) using methylene blue inhibits the viability of the biofilm produced by *Candida albicans*. *Photodiagnosis Photodynamic Ther.* 2019; **26**, 316-23.

[45] I Ahamad, F Bano, R Anwer, P Srivastava, R Kumar and T Fatma. Antibiofilm activities of biogenic silver nanoparticles against *Candida albicans*. *Front. Microbiol.* 2022; **12**, 741493.

[46] M Jalal, MA Ansari, MA Alzohairy, SG Ali, HM Khan, A Almatroudi and MI Siddiqui. Anticandidal activity of biosynthesized silver nanoparticles: effect on growth, cell morphology, and key virulence attributes of Candida species. *Int. J. Nanomedicine* 2019; **14**, 4667-79.

[47] MMJ Arsène, PI Viktorovna, M Alla, M Mariya, SA Nikolaevitch, AKL Davares, ME Yurievna, M Rehailia, AA Gabin, KA Alekseevna, YN Vyacheslavovna, ZA Vladimirovna, O Svetlana and D Milana. Antifungal activity of silver nanoparticles prepared using Aloe vera extract against *Candida albicans*. *Vet. World* 2023; **16**, 18-26.

[48] T Bruna, F Maldonado-Bravo, P Jara and N Caro. Silver nanoparticles and their antibacterial applications. *Int. J. Mol. Sci.* 2021; **22**, 7202.

[49] PR More, S Pandit, AD Filippis, G Franci, I Mijakovic and M Galdiero. Silver nanoparticles: Bactericidal and mechanistic approach against drug resistant pathogens. *Microorganisms* 2023; **11**, 369.